Impact of *Xylella fastidiosa* subspecies *pauca* in European olives

Kevin Schneider[a,1], Wopke van der Werf[b], Martina Cendoya[c], Monique Mourits[a], Juan A. Navas-Cortés[d], Antonio Vicent[c], and Alfons Oude Lansink[a]

[a]Business Economics Group, Wageningen University, 6700 EW, Wageningen, Netherlands; [b]Centre for Crop Systems Analysis, Wageningen University, 6700 AK, Wageningen, Netherlands; [c]Centre de Protecció Vegetal i Biotecnología, Institut Valencià d'Investigacions Agràries, 46113 Moncada (Valencia), Spain; and [d]Institute for Sustainable Agriculture, Spanish National Research Council (CSIC), 14004 Córdoba, Spain

Edited by Charles Perrings, Arizona State University, Tempe, AZ, and accepted by Editorial Board Member Simon A. Levin March 3, 2020 (received for review July 16, 2019)

Xylella fastidiosa **is the causal agent of plant diseases that cause massive economic damage. In 2013, a strain of the bacterium was, for the first time, detected in the European territory (Italy), causing the Olive Quick Decline Syndrome. We simulate future spread of the disease based on climatic-suitability modeling and radial expansion of the invaded territory. An economic model is developed to compute impact based on discounted foregone profits and losses in investment. The model projects impact for Italy, Greece, and Spain, as these countries account for around 95% of the European olive oil production. Climatic suitability modeling indicates that, depending on the suitability threshold, 95.5 to 98.9%, 99.2 to 99.8%, and 84.6 to 99.1% of the national areas of production fall into suitable territory in Italy, Greece, and Spain, respectively. For Italy, across the considered rates of radial range expansion the potential economic impact over 50 y ranges from 1.9 billion to 5.2 billion Euros for the economic worst-case scenario, in which production ceases after orchards die off. If replanting with resistant varieties is feasible, the impact ranges from 0.6 billion to 1.6 billion Euros. Depending on whether replanting is feasible, between 0.5 billion and 1.3 billion Euros can be saved over the course of 50 y if disease spread is reduced from 5.18 to 1.1 km per year. The analysis stresses the necessity to strengthen the ongoing research on cultivar resistance traits and application of phytosanitary measures, including vector control and inoculum suppression, by removing host plants.**

species distribution models | radial range expansion | simulation | perennials | pest risk assessment

Xylella fastidiosa (*Xf*) is a bacterium from the family *Xanthomonadaceae* and was first described by Wells et al. (1). The list of host plants for *Xf* currently comprises 563 plant species from the Americas, Europe, the Middle East, and Asia (2). In the European Union (EU), at least 84 host plants for *Xf* have been identified (3). This species is considered one of the most dangerous plant-pathogenic bacteria worldwide (2, 4). The bacterium is naturally transmitted by insect vectors, which feed on the xylem of host plants (5, 6). If expressed in susceptible plant hosts, symptoms of *Xf* include, among others, leaf marginal necrosis, leaf abscission, dieback, delayed growth, and death of plants through the obstruction of the xylem and a lack of sufficient water flow through the host (7, 8). The multiplication of the bacteria with the associated clogging of the xylem will first result in declining yields and reduced fruit quality due to a decrease in water and nutrient flow (9). Eventually, this shortage will result in the host's death (10).

In 2013, *Xf* subspecies (subsp.) *pauca* (*Xfp*) was detected in *Olea europaea* (olive), *Nerium oleander* (oleander), and *Prunus dulcis* (almond) in Italy (11). The detection led to the enactment of control measures, including vector control and tree felling. The latter resulted in great societal unrest in the affected region (12, 13). Unfortunately, the size of the area currently affected and the hidden reservoir of symptomless, but infectious, host plants is likely to hinder any attempts of disease eradication (14). Furthermore, recent studies suggest that the tight network of olive orchards in Apulia (Italy) can be expected to serve as a European reservoir of *Xfp* (15). Nevertheless, the removal of infected trees and vector control along the border of the infected area may act as a cordon sanitaire reducing disease spread.

Currently in the EU, *Xf* is present in Italy, France, Spain, and Portugal, including the subsp. *pauca*, *multiplex*, and *fastidiosa* (16). Since there is no practical cure for *Xf* under field conditions (17, 18), control strategies applied in the EU focus on eradication or containment of the disease by host removal, vector control, and restrictions on the production and movement of plant materials for planting. Research efforts are currently targeting the identification of resistance traits and biological control (19–27). The use of nonhost species or resistant cultivars of host species seems the most feasible and promising long-term strategy to adapt to *Xf* in affected regions (4, 9). Important advances have been made with regard to the identification of resistant cultivars. In particular, symptom expression in the olive varieties FS-17 and Leccino is drastically reduced compared to other cultivars. The enacted regulatory measures prohibit replanting of hosts within the infected zone. Exceptions were made for FS-17 and Leccino,

Significance

Xylella fastidiosa **is one of the most dangerous plant-pathogenic bacteria worldwide. Regulatory measures were enacted in response to the detection of the subsp.** ***pauca*** **(*Xfp*) in Italian olives in 2013, but the current impact is nevertheless major. We developed a spatially explicit bio-economic model to compute potential future economic impact of the *Xfp* strain. Uncertainty on spread is accounted for by simulating different scenarios. The majority of orchards were found to be within climatically suitable territory. Even under slow disease spread and the ability to replant with resistant cultivars, projections of future economic impact in affected countries run in the billions of Euros. Our findings highlight the importance of minimizing disease spread and implementing adaptation measures in affected areas.**

Author contributions: K.S., W.v.d.W., M.C., M.M., J.A.N.-C., A.V., and A.O.L. designed research; K.S., M.C., and J.A.N.-C. performed research; K.S., W.v.d.W., M.C. and J.A.N.-C. analyzed data; and K.S., W.v.d.W., M.M., A.V., and A.O.L. wrote the paper.

The authors declare no competing interest.

This article is a PNAS Direct Submission. C.P. is a guest editor invited by the Editorial Board.

Data deposition: Data and R scripts are available in Zenodo (https://doi.org/10.5281/zenodo.3672794).

[1]To whom correspondence may be addressed. Email: kevin.schneider@wur.nl.

This article contains supporting information online at https://www.pnas.org/lookup/suppl/doi:10.1073/pnas.1912206117/-/DCSupplemental.

First published April 13, 2020.

which are currently the only olive cultivars that may be replanted in the infected zone (28).

Here, we develop a spatially explicit bio-economic model that accounts for disease spread and economic characteristics of olive-cultivation systems in different European countries (29). The model projects impact for Italy, Greece, and Spain, as these countries account for around 95% of the European production (30). Impact is computed over a 50-y time horizon employing a suite of models. The climatically suitable territory is assessed by using an ensemble prediction based on 10 species distribution models (SDMs). The spatial distribution of olive orchards is obtained from land-cover data. The disease spread is simulated by using a cellular automaton model with mixed neighborhood processes (rook's and queen's case contiguity) to approximate a radial spread process at spread rates obtained from expert knowledge elicitation (EKE). We account for the uncertainty in the annual rate of dispersal by using three quantiles of the expert-elicited distribution of spread rates (16). An economic model is developed to compute impact to growers as discounted foregone profits and losses in investment due to the premature death of infected trees. Additional profits to nonaffected growers, as a result of price responses to changes in the European supply, are accounted for. For all disease-spread scenarios, two economic scenarios are explored. In the first, production is assumed to cease once production in an orchard becomes unprofitable due to the disease. In the second, infected orchards are replanted with a resistant cultivar. These two extremes bracket the plausible range of impact. The bio-economic scenarios are compared to a baseline in which *Xfp* is absent. The difference between both economic scenarios approximates the benefit from resistant cultivars.

Consequently, this study derives various insights. First, we report on the climatic suitability of the European olive-production sites for establishment and spread of *Xf*. Second, we explore the bandwidth of economic impact that results from uncertainty regarding the annual rate of dispersal. Here, we also compare results for different spread rates to provide insights on the economic benefit that might be secured through means of reducing the rate of spread, such as vector control and host removal. Third, we analyze economic impact from possible introductions into Greece and Spain. This allows us to identify high-risk areas for disease introduction and establishment and discuss differences between countries in the sensitivity of results with regard to the uncertainty on the annual rate of dispersal, as well as compare the magnitude of the potential future economic impact between Italy, Greece, and Spain.

The uncertainty on various aspects was taken into consideration. First, while previous work explored the importance of long-distance jumps for the spread of *Xfp* (31), data to accurately parameterize such jumps are currently not available. Therefore, our spread model simplifies the dispersal process into a composite spread, comprising local dispersal and probabilistic jumps. Second, we make use of country-wide averages of prices and operational costs per ton of olives due to the unavailability of data at finer spatial resolution. Third, the economic model intends to derive insights into the potential impacts to olive growers. Processors and consumers are not included into the analysis. We discuss consequences of this simplification and address expected market effects in more detail below. Fourth, changes in fruit quality due to *Xfp* are not considered. Reductions in oil yield per ton of olives may reduce the willingness to pay on the side of processors. Consequently, the periods for which continued production on infected plots is profitable would be shortened, and impacts would be slightly higher as a result. Fifth, for the replanting scenario, we assume that the replanted trees are fully resistant or tolerant to the pathogen and produce the same profits as their susceptible predecessors. While full resistance is achievable, partial resistance or reductions in full-bearing yields might be the outcome of breeding for resistance or tolerance. Lastly, we present an economic best-case scenario in which infected orchards are replanted with resistant equivalents. Many of the olive-tree cultivars have been inherited from generation to generation over the last centuries. Arguably, these trees represent a sizable cultural heritage value for many growers and other citizens across Europe (12, 13). Furthermore, olive orchards provide a landscape value, which benefits other sectors such as tourism (32). Due to the difficulties of quantifying cultural heritage and landscape values in monetary terms, we omit these aspects from our analysis. Nevertheless, this study intends to contribute to a more informed discussion among stakeholders by exploring the direct economic impact that can be expected from *Xfp* for European olive growers.

Results

The results on climatic suitability were obtained in the form of a continuous variable, which can range from zero to one for a given location in Europe. The continuous scores were converted to a binary prediction (suitable or unsuitable) based on three different thresholds. The thresholds are numerical cut-offs such that locations with higher values are classified as suitable. A threshold of 0.165 (T1) was used to ensure that the model correctly predicted at least 90% of the locations in which *Xf* was confirmed to be present as suitable (90% sensitivity). A threshold of 0.132 (T2) maximizes the sum of the accuracy of predicting occupied sites to be suitable and unoccupied sites to be unsuitable (i.e., maximizing the sum of sensitivity and specificity), and a value of 0.093 (T3) minimizes the difference between the accuracy of predicting occupied sites to be suitable and unoccupied sites to be unsuitable (i.e., minimum difference between sensitivity and specificity) (16). Spatially explicit information on the distribution of European olive orchards was incorporated via the Coordination of Information on the Environment (CORINE) land-cover map, which was aggregated to a 1-km resolution. The ensemble prediction from the SDMs suggests that for the three thresholds between 95.5 and 98.9%, 99.2 and 99.8%, and 84.6 and 99.1% of the national area of production falls into climatically suitable territory in Italy, Greece, and Spain, respectively (see Fig. 1 *A*–*C*).

The radial range expansion model requires a point of origin and simulates radial dispersal around this point, assuming that all climatically suitable cells within this range may be affected. In our model, spread of the disease is realized through cell-to-cell transmissions. While these transmissions require that the invaded cells are climatically suitable, they do not depend on olives to be present. Consequently, our spread model simulates temporal as well as spatial spread by acknowledging the spatially explicit distribution of olive-production sites, under the assumption that alternative hosts assist dispersal through climatically suitable habitat. There is still very incomplete knowledge on the rate of spread of *Xfp* (31, 33). While monitoring data on the outbreak in Apulia are available, the sampling design in the region drastically changed over time since the first detection. This presumably is related to a change in priorities of authorities from detection to containment of the disease. Consequently, estimating epidemiological parameters is severely aggravated if not impossible. In addition, the observed epidemic in Apulia is likely to be a worst-case scenario due to the tight network of orchards and the abundance of suitable vectors (15, 31). Therefore, extrapolating estimated parameters for Apulia to continental Europe would be questionable.

To take the uncertainty on the spread rate into account, we utilized the 5th, 50th, and 95th percentiles of a distribution of spread rates obtained by formal EKE. The quantiles correspond

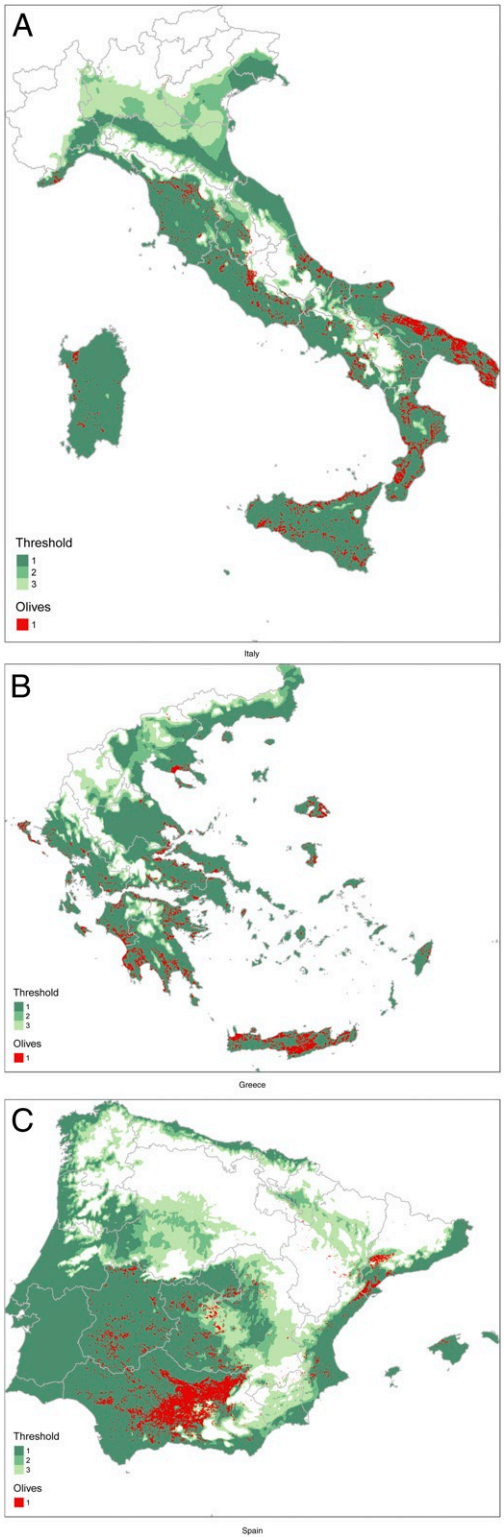

Fig. 1. Binary suitability maps and olive-production sites in Italy (*A*), Greece (*B*), and Spain (*C*).

to a rate of radial range expansion of 1.10 (RR05), 5.18 (RR50), and 12.35 (RR95) km per year (16). The elicited rates account for the heterogeneous landscape in Europe, differences in vector abundance, and application of control measures, as is currently done. Long-distance jumps due to plant trade were not considered in the spread simulations within countries. However, they were accounted for when studying introductions into Spain or Greece (see below). For Italy, we analyzed nine different spread scenarios resulting from the combination of the three spread rates and three thresholds for the binary climatic suitability map. As the elicited rates intend to gauge the pace of spread beyond the current extent, we classified the extent known to be affected in 2019 as infected at the starting point of our modeling time horizon. Subsequently, spread was simulated beyond the infected zone for the three different rates (Fig. 2). For Greece and Spain, the uncertainty on the potential point of introduction of the disease was accounted for by randomly infecting one olive cell within climatically suitable territory. For every suitability threshold, 1,000 points of introduction were generated per country. Subsequently, for each point of introduction spread was simulated for RR05, RR50, and RR95. In turn, 9,000 spread scenarios were analyzed for Greece and Spain, respectively. A visualization of all generated points of introduction is provided in *SI Appendix*, Fig. S1.

For RR05, around 22% of the Italian area of production was affected at the end of the 50-y time horizon. The suitability thresholds did not alter these results, because cells within the extent reached fall into suitable territory, regardless of the chosen threshold. For RR50, depending on the climatic suitability threshold, between 50.3 and 52.9% of the Italian area of production was infected at the end of the 50-year time horizon. For RR95, depending on the climatic suitability threshold between 68.6 and 75.3% of the Italian area of production was infected at the end of the 50-y time horizon. For Greece, on average across the random points of introduction, depending on the climatic suitability threshold, between 7.7 and 8.0%, 28.2 and 28.9%, and 34.5 and 38.5% of the national area of production was infected for RR05, RR50, and RR95, respectively. For Spain, on average across the random points of introduction, depending on the climatic suitability threshold, between 11.4 and 12.3%, 62.9 and 69.6%, and 74.5 and 94.8% of the national area of production was infected for RR05, RR50, and RR95, respectively.

The uncertainty on the point of introduction of the disease in Greece and Spain sensitively influenced the area reached by the pathogen and, in turn, the economic impact. Irrespective of the annual rate of dispersal, the share of the national area infected was found to differ substantially across the randomized points of introduction (*SI Appendix*, Figs. S3, S5, and S7). For Greece, introductions into Crete, Attica, and western or central Greece resulted in sizable shares of the national area infected, whereas introduction onto islands in the northern or southern Aegean as well as central Macedonia remained isolated from the country's main areas of olive production. For Greece, the consequences of differences in the annual rate of spread were not as pronounced as for the other two countries. The Greek main areas of production are divided between mainland regions and Crete. The sea, as a natural barrier for spread, prevented the epidemic from reaching more than 38.5% of the national area of production, on average, across the random points of introduction, even for larger annual rates of spread. For Spain, the different climatic thresholds not only influenced the share of the national area of production within climatically suitable territory more strongly compared to the other two countries, but also more sensitively determined the area reached by the epidemic compared to Italy and Greece. The spatial continuity of the climatically suitable area in central Spain influenced whether introductions into Catalonia and the Valencian Community were contained within those regions or whether they spread over Castilla La Mancha into the country's main area of olive production in Andalusia (Fig. 1*C*). Visualizations of changes in high-risk points of introduction depending on the suitability threshold are provided in *SI Appendix*, Figs. S4 and S6.

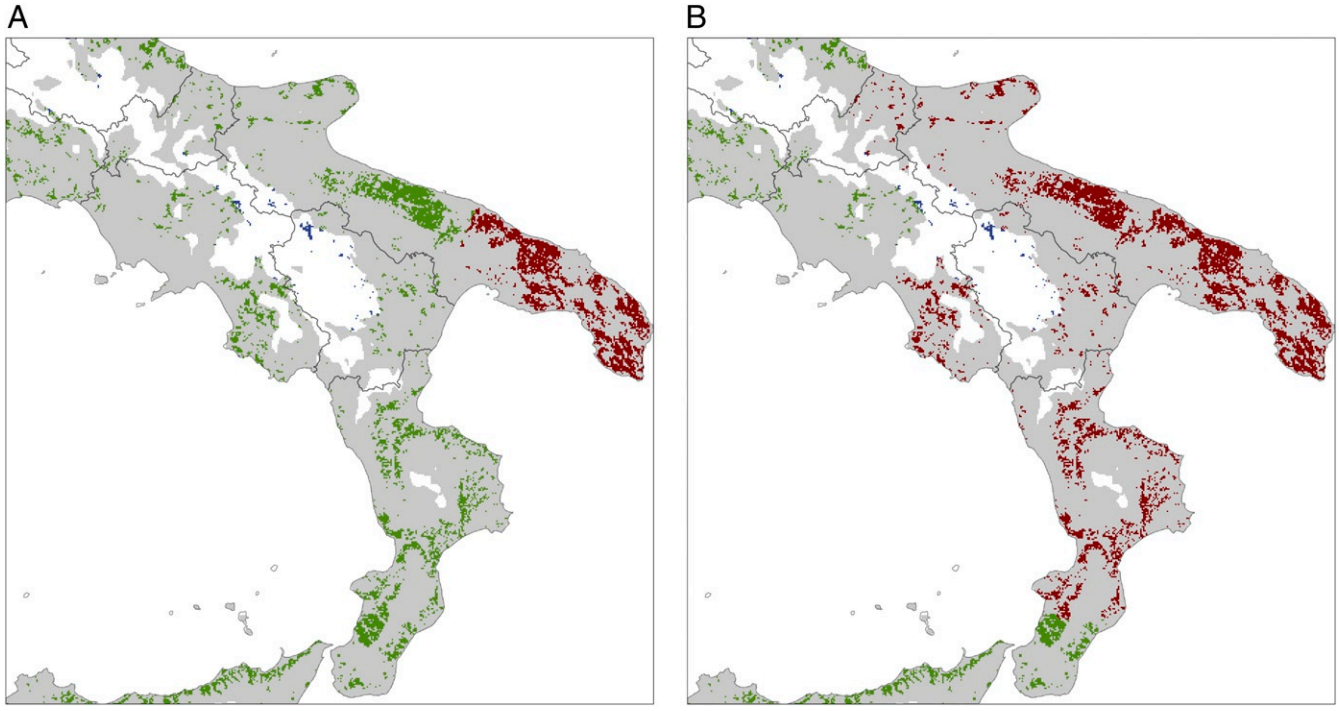

Fig. 2. Simulated geographical distribution of *Xfp* in years 5 (*A*) and 50 (*B*) with the median of the elicited rate of radial range expansion (5.18 km per year) and a climate suitability threshold of 0.132 in the ensemble SDM. Gray depicts suitable territory. Blue depicts nonsuitable olives. Green depicts suitable olives. Red depicts infected olives.

The spread scenarios resulted in different extents of the European olive production lost and, in turn, different price responses following reductions in European supply if replanting is not feasible. For spread in Italy, depending on the climatic suitability threshold, around 5.5%, 12.6 to 13.2%, and 17.7 to 18.9% of the European supply was lost in year 50 for RR05, RR50, and RR95, respectively. Consequently, prices were estimated to increase by approximately 2.9%, 6.5 to 6.9%, and 9.2 to 9.8% across Europe. For spread in Greece, depending on the climatic suitability threshold, around 1.4%, 5.3 to 5.4%, and 6.7 to 7.4% of the European supply was lost in year 50 for RR05, RR50, and RR95, respectively. As a result, prices were estimated to increase by 0.7%, 2.8%, and 3.8% across Europe. For spread in Spain, depending on the climatic suitability threshold, 5.4 to 5.8%, 32.4 to 35.4%, and 40.8 to 50.6% of the European supply was lost in year 50. Prices were estimated to increase by 2.8 to 3.0%, 16.8 to 18.4%, and 21.2 to 26.3% across Europe.

Table 1 depicts the economic impact over the course of 50 y in terms of present value. For Italy, the differences in the economic results for the different climatic suitability thresholds were negligible. To improve readability, only the results for T2 are presented. Results for all thresholds can be found in *SI Appendix*, Table S2. For Italy, total impact ranged between 1.86 billion Euros for RR05 and 5.17 billion Euros for RR95 if replanting is not feasible. Notably, the increase in producer prices following reductions in Italian supply positively affected Greek and Spanish growers. Depending on the spread rate and, in turn, the magnitude of the Italian supply reduction, the additional profits ranged between 0.68 billion and 1.59 billion Euros for Greece and 1.71 billion and 3.99 billion Euros for Spain. Summed over the countries, additional profits to growers ranged between 0.74 billion and 1.02 billion Euros. Under the replanting scenario, impact in Italy ranged between 0.59 billion and 1.57 billion Euros. The recovery of the Italian supply diminished the price increase, which resulted in reduced additional profit flows for Greek and Spanish growers when compared to the scenario without replanting. Nevertheless, the additional profits ranged between 0.10 billion and 0.24 billion Euros for Greece and 0.26 billion and 0.62 billion Euros for Spain. Summed over the three countries, losses in profits ranged between 0.02 billion and 0.1 billion Euros. Regardless of the economic scenario, between 0.21 billion and 0.61 billion Euros' worth of investments were lost due to the premature death of trees in Italy. The rainfed-intensive and rainfed-traditional cropping systems were responsible for most of these losses, with shares on the losses in investment of 28% and 27%, respectively. The benefit of resistant cultivars to Italy ranged between 1.27 billion to 3.60 billion Euros. Evidently, nonaffected producers would benefit if Italian growers were not able to recover their supply using resistant trees.

For Greece and Spain, all impacts presented below represent averages across the 1,000 random points of the future introduction scenarios. The distributions of all economic results for each spread scenario can be found in *SI Appendix*, Figs. S8 and S9. For Greece, total impact ranged between 0.21 billion Euros for RR05 and 1.94 billion Euro for RR95 if *Xfp* is introduced and replanting is not feasible. Again, the increase in producer prices following reductions in Greek supply positively affected producer profits in the other two included countries. Depending on the spread rate and, in turn, the magnitude of the Greek supply reduction, the additional profits ranged between 0.18 billion and 1.60 billion Euros for Spain and 0.09 billion and 0.76 billion Euros for Italy. Summed over the countries, additional profits to growers ranged between 0.10 billion and 0.71 billion Euros. Under the replanting scenario, Greek impacts ranged between 0.09 billion and 0.58 billion Euros. The recovery of the Greek supply diminished the price increase, which reduced the additional profits to the other countries compared to the scenario where replanting is not feasible. The additional profits ranged between 0.03 billion and 0.19 billion Euros for Spain and 0.01 billion and 0.09 billion Euros for Italy.

Table 1. Economic impact over 50 y in billion Euros

	Without replanting						With replanting							Benefits of resistance		
	Total impact			Change in profits			Total impact			Change in profits			Lost			
	EL	ES	IT	EL	ES	IT	EL	ES	IT	EL	ES	IT	investment	EL	ES	IT
Xfp spread in Italy																
—RR05	0.68	1.71	−1.86	0.68	1.71	−1.65	0.10	0.26	−0.59	0.10	0.26	−0.38	−0.21	−0.58	−1.45	1.27
—RR50	1.04	2.61	−3.15	1.04	2.61	−2.75	0.17	0.42	−1.05	0.17	0.42	−0.65	−0.40	−0.87	−2.18	2.10
—RR95	1.59	3.99	−5.17	1.59	3.99	−4.56	0.24	0.62	−1.57	0.24	0.62	−0.96	−0.61	−1.34	−3.37	3.60
Xfp spread in Greece*																
—RR05	−0.21	0.18	0.09	−0.17	0.18	0.09	−0.09	0.03	0.01	−0.04	0.03	0.01	−0.04	0.13	−0.15	−0.07
—RR50	−1.08	0.89	0.42	−0.89	0.89	0.42	−0.37	0.12	0.06	−0.18	0.12	0.06	−0.19	0.71	−0.77	−0.37
—RR95	−1.94	1.60	0.76	−1.65	1.60	0.76	−0.58	0.19	0.09	−0.29	0.19	0.09	−0.29	1.36	−1.41	−0.67
Xfp spread in Spain*																
—RR05	0.21	−0.71	0.25	0.21	−0.53	0.25	0.05	−0.39	0.06	0.05	−0.21	0.06	−0.17	−0.16	0.32	−0.19
—RR50	1.90	−7.83	2.27	1.90	−6.55	2.27	0.37	−2.93	0.44	0.37	−1.65	0.44	−1.27	−1.53	4.90	−1.83
—RR95	3.76	−16.86	4.50	3.76	−14.74	4.50	0.61	−4.98	0.73	0.61	−2.85	0.73	−2.12	−3.15	11.88	−3.77

EL, Greece; ES, Spain; IT, Italy. All results are for a climatic suitability threshold of 0.132.
*Averaged over all random points of introduction.

Regardless of the economic scenario, between 0.04 billion and 0.29 billion Euros' worth of investments were lost due to the premature death of trees in Greece. The irrigated-intensive and irrigated-traditional cropping systems were responsible for most of these losses, with shares on the total losses in investment of 35% and 27%, respectively. The benefit of resistant cultivars to Greece ranged between 0.13 billion and 1.36 billion Euros. For Spain, total impact ranged between 0.71 billion Euros for RR05 to 16.86 billion Euros for RR95 if *Xfp* is introduced and replanting is not feasible. Again, the increase in producer prices following reductions in Spanish supply positively affected the other two included countries. Depending on the spread rate and, in turn, the magnitude of the Spanish supply reduction, the additional profits ranged from 0.21 billion to 3.76 billion Euros for Greece and 0.25 billion to 4.50 billion Euros for Italy. Summed over the countries, foregone profits to growers ranged between 0.07 billion and 6.48 billion Euros. Under the replanting scenario, Spanish impact ranged between 0.39 billion and 4.98 billion Euros. The recovery of the Spanish supply diminished the price increase, which reduced the additional profits to the other countries compared to the scenario where replanting is not feasible. The additional profit flows ranged from 0.05 billion to 0.61 billion Euros for Greece and 0.06 billion to 0.73 billion Euros for Italy. Summed over the countries, foregone profits to growers ranged between 0.10 billion and 1.51 billion Euros. Regardless of the economic scenario, between 0.17 billion and 2.12 billion Euros' worth of investments were lost due to the premature death of trees in Spain. The irrigated-traditional and rainfed-traditional cropping systems were responsible for most of these losses, with shares on the total losses in investment of 32% and 22%, respectively. The benefit of resistant cultivars to Spain ranged between 0.32 billion and 11.88 billion Euros.

Evidently, the magnitude of the economic impact differed between the three countries. This can be attributed to the differences in the total area of production, distribution of this area into the different cropping systems, and country-specific profitability of olive production per hectare. However, as described above, spatial characteristics of the three countries crucially determined the area of production that was reached by *Xfp* within the time horizon for the different spread rates. On average, across the random points of introduction, the natural barriers around areas of production in Greece prevented impacts above 1.94 billion Euro. Due to the spatial continuity of the climatically suitable territory in Spain and the spatial concentration of olive production in Andalusia, impact drastically exceeded the impact computed for Italy for RR50 and RR95. The calculated impacts for Spain and Greece are contingent on introduction of the pathogen within these countries at the start of the time horizon.

The economic benefit that might be secured by reducing the annual rate of spread was found to differ among the evaluated countries. For Italy, a reduction in the rate of spread from 5.18 to 1.1 km per year was found to reduce the overall impact by around 41% and 44% in the scenarios without replanting and with replanting, respectively. In other words, around 1.29 billion or 0.46 billion Euros would be saved. For Greece and Spain, the economic benefit from reducing the annual rate of dispersal is larger with reductions in the overall impact by around 81% and 91%, respectively. This corresponds to economic savings of 0.87 billion Euros for Greece and 7.12 billion Euros for Spain if the rate of spread would be reduced from 5.18 to 1.1 km per year and replanting is not feasible. The difference in the sensitivity of the results with regard to the annual spread rate can be explained by the different types of starting conditions. For Italy, we initiated spread beyond the currently known infected zone, which already comprises 17% of the national area of production. For Greece and Spain, the simulations were initiated on a randomly generated suitable olive cell. In turn, the area infected within the time horizon is more sensitively influenced by the annual rate of spread, which resulted in the differences in the economic benefit from delaying the further dispersal of the disease.

A global sensitivity analysis of the economic model based on spread in Italy using variance decomposition showed that only a few out of 31 parameters had statistically significant first-order indices at the 5% level. Uncertainty regarding the prices and costs per ton of olives in Italy and the discount rate, as well as the changes in yield and operational costs due to *Xfp* were found to sensitively influence the results. Table 2 depicts the first- and total-order sensitivity indices for the statistically significant parameters. Detailed results for all parameters can be found in *SI Appendix*, Tables S3–S8. Price per ton of olives was most influential and caused 72% and 76% of the variance in impact with and without replanting, respectively. The profitability per ton of olives will crucially determine the profits foregone and, in turn, the total impact. This indicates that the effects of the observed empirical variation in prices and costs outweigh the uncertainty in replanting costs as well as other orchard-specific parameters, such as the longevity of the cropping systems. Research on the expected annual decline of yield following infection with *Xfp* as well as data on changes in operational costs following infection would benefit further modeling efforts.

Table 2. First- and total-order sensitivity indices of significant economic parameters without replanting (S1), with replanting (S2), and resistance benefits (RB) for impact in Italy

	First order			Total order		
Parameter	S1	S2	RB	S1	S2	RB
Price Italy	0.664	0.619	0.480	0.717	0.756	0.629
Costs Italy	0.165	0.142	0.117	0.169	0.223	0.149
Discount rate	0.033		0.074	0.070		0.160
Yield decline			0.039			0.191
Cost change			0.039			0.163

Discussion

While impacts were not sensitively influenced by the climatic limits for Italy and Greece, the different climatic suitability thresholds did more strongly influence the maximum extent and the dispersal path of *Xfp* in Spain. Locations and timing of future introductions of the pathogen, if any, are highly uncertain. More research on the climatic suitability for *Xf* in Castilla La Mancha could provide important information on the spatial continuity of the suitable area. This continuity will crucially determine whether nondetected introductions into coastal areas can be expected to be contained by unsuitable climatic barriers or whether the disease is able to relatively quickly spread into the main olive-production sites in Andalusia.

Our analysis revealed that sizable impact can be expected from new introductions of *Xfp* into olive-dense production areas, irrespective of the annual rate of spread. This stresses the need for growers to be vigilant and promptly report possible infections to the national plant-protection organizations. Unfortunately, the ability to promptly report introductions and initiate actions to prevent further dispersal crucially depends on the length of the asymptomatic period following infection.

The results show that the economic benefit that might be secured through reducing the rate of dispersal depends on the existence of natural barriers for disease spread and the distribution of olive-production sites in a country. Once *Xfp* is well established in an area and has reached a large geographical extent, eradication is considered not practical (15). Therefore, phytosanitary regulations focus mainly on reducing the rate of disease spread by felling trees and suppressing vectors at the border of the infected area (28, 34). In particular for Italy and Spain, our results suggest sizable benefit from reducing the annual spread rate. This indicates that current phytosanitary measures to reduce disease spread via inoculum suppression and vector control are of great importance. Further efforts to identify additional effective measures, as done in ref. 18, are called for. However, our results also indicate that introductions into islands of Greece might be managed by early detection, containment, and eradication. While reductions in the spread rate still resulted in a sizable benefit in Greece, the natural barriers contained even spread at a larger rate comparatively well. This could render eradication and containment efforts more feasible. Hence, countries with a more continuous climatically suitable territory and a concentration of olive-production sites seem to benefit more strongly from means of reducing the annual spread rate. Certainly, more work is needed to provide a sound analysis of territory-based control strategies against *Xfp*. The development of vector-based spread models will greatly benefit future work on this (35).

The planting of resistant cultivars or the substitution of olive production by other land uses seems the most feasible and promising strategy to control *Xf* in those regions where the pathogen is no longer eradicable (4, 9). Current regulations allow planting of two resistant olive cultivars within the infected zones in the containment areas in Italy (28). Our analysis revealed a clear benefit, for affected countries, of replanting with resistant varieties. The olive cultivars FS-17 and Leccino present promising points of departure (19, 20, 23, 25). However, more research is needed on their performance under field conditions in different cropping systems and different parts of Europe. To prevent landscapes with genetically uniform trees, further breeding efforts are crucial.

Earlier studies on perennials did not account for the possibility of a continued production on partially infected plots (36). We found that continuing cultivation for a limited period was economically rational. However, early clearing of infected trees might limit the spread of the disease (37). Therefore, the social benefits derived from the removal of entire infected orchards can be viewed as a public good, suggesting that the costs of eradication warrant compensation from authorities (38). The analysis revealed that our conservative assumption on the annual decline (increase) of yield (operational cost) by 10% resulted in negative profit margins within 2 to 4 y after first infection, depending on the country and cropping system. In turn, commercial farmers can be expected to cease production relatively quickly following symptom expression of *Xfp*. This might increase the European loss in production beyond what is expected when solely focusing on the biological yield decline (16). If olives harvested from infected trees result in lower oil yield per ton of olives, willingness to pay on the side of the processor might be reduced, which would slightly increase impacts by shortening the periods for which continued production under infection is profitable.

Our analysis focused on the impacts to growers to narrow down on the intersection of biology and economics. By taking the cropping-system-specific conditions into account, we were able to simulate the replanting scenario and derive impacts which arise solely through the premature death of trees. In general, invasive species tend to result in reductions in yield, which, if the extent of the epidemic is sufficiently large, result in changes in the country's total production. In cases in which the affected country is a significant contributor to the European (or world) supply, the reduction in the production is likely to result in an increase in price (39). As highlighted within this analysis, higher producer prices will benefit nonaffected growers (40–42). Most olives are used as an input for processing into olive oil. In turn, the simulated price increase would result in higher costs of production for oil processors. This could affect the consumer price for olive oil. However, the degree to which the change in production costs could be transferred to consumers and the degree to which higher consumer prices for olive oil would be transmitted back to olive growers depends on magnitude, speed, and asymmetry of price transmissions in the supply chain (43). Among other aspects, these factors are influenced by the existence of market power of processors (44), as well as the consumers' willingness to switch to alternative products. Future work could build on the framework developed within this study and narrow down on modeling these supply chain-related aspects. This could add insights into the potential impacts to processors, consumers, and competing markets.

Some of our assumptions may be too optimistic. First, the profit flows understate the value generated through olive processing. If the level of analysis is extended to olive oil, the economic impact would be greater due to the larger profit margins in the oil production (45). In 2017, the production value of olives was around 2.4 billion Euros, whereas the production value of olive oil was around 6.7 billion Euros (46). Second, farms were assumed to be able to replant. However, the olive sector in Europe is characterized by relatively small-scale farming, and some farms may not have the financial means for replanting (45, 47). In our study, resistant cultivars were defined as those not suffering reductions in yield or quality when planted in an infected area. This applies both to completely resistant cultivars, where the host and the pathogen are incompatible,

or completely tolerant cultivars, where the host is infected but without yield loss (48). While full resistance is achievable, partial resistance or reductions in full-bearing yields might be the outcome of breeding efforts. In addition, tolerant cultivars remain hosts for the pathogen and are inoculum reservoirs (49), which might support disease spread. Lastly, vigilant growers might aim to stay ahead of the disease by additional monitoring efforts and preventive measures prior to their orchards being infected. Consequently, associated increases in operational costs due to these preventive measures outside of the radial range of infection would increase total impact beyond what was computed here.

Replanting sometimes centuries-old or even millennial trees by young trees has severe consequences in terms of cultural heritage and provision of a landscape that is attractive for tourism and recreation. Quantifying these losses in monetary terms was not within the scope of this analysis. Furthermore, the slow development of olive orchards can be expected to result in considerable nurturing costs. Additional income-support schemes might be necessary to ensure that farmers remain financially capable to nurture the orchards back into a productive state that contributes to cultural heritage and an attractive landscape in the affected areas.

Xfp is known to affect various economically important hosts, including, besides olives, also cherries and almonds. Additional assessments on other host species would inform the discussion on risks associated with new introductions of *Xf* or the further dispersal of the strain detected in Italy. Certainly, the importance of the European wine sector calls for an assessment of subsp. *fastidiosa* in grapevine. The modeling framework developed within this study could very well be used for this. The overall potential impact of *Xf* in Europe may thus far exceed the impact evaluated here for the subsp. *pauca* in one host, olive.

Materials and Methods

Climatic Suitability Map. SDMs explore the relationship between geographical occurrences of species and environmental variables (50, 51). SDMs draw statistical inference on drivers of species ranges from a snapshot of occurrence data by finding statistical correlations between species' distributions and environmental factors. We make use of occurrence data of *Xf* from the update of the *Xf* host database (2), local datasets of outbreaks in Italy, France and Spain which were obtained from the national plant-protection organizations (i.e., Osservatorio Fitosanitario Regione Puglia, Italy; Servicio de Sanidad Vegetal, Generalitat Valenciana, Spain; Conselleria de Medi Ambient, Agricultura i Pesca del Govern de les Illes Balears, Spain; and Bureau de la Santé des Végétaux, Ministère de l'Agriculture et de l'Alimentation, France) as well as recent records of *Xf* in Porto, Tuscany, and Hula Valley (52–54). The presence records were filtered in three ways: first, by selecting only records from infection observed under natural inoculum pressure either during surveys or research activities on natural habitat, thereby omitting records from greenhouse, screenhouse, or interceptions; second, by selecting records with precise geographic coordinates; and third, by only using records with confirmed positives. To reduce spatial autocorrelation, the presence records were further submitted to a spatial-filtering approach. In this procedure, the presence records were randomly selected according to a minimum nearest-neighbor distance of at least 5 km between each locality. This distance is equal to the spatial resolution used for the climatic data. The procedure was repeated four times, obtaining four different spatially filtered datasets. We generated weighted pseudo-absence data to simulate a prevalence of 0.1. To explore and reduce the uncertainty of the random sampling, we repeated this process four times to generate four pseudo-absence datasets per model replication. Climate data were obtained from Chelsa Climatology (55). The data ranged from 1979 to 2013 and are a downscaled version of the European Centre for Medium-Range Weather Forecasts Reanalysis Interim (ERA-Interim) global circulation model. We used data at a 5-km resolution. Nineteen bioclimatic variables were analyzed, out of which nine were included into the prediction after controlling for multicollinearity (variance inflation factor <10). The ensemble prediction followed the methodology described within ref. 16. However, for this study, we refined the spatial prediction from a resolution of 10 to 5 km. We made use of 10 modeling techniques, namely, bioclim, boosted and regression trees, classification and regression trees, domain, generalized additive models, multivariate adaptive regression splines, maximum entropy, random forest, recursive partitioning, and regression trees and support vector machines. Model performance was evaluated by using the true skill statistic (56). In total, we computed 800 models comprising four spatially filtered datasets, four pseudo-absence sampling replicates, 10 modeling techniques, and five cross-validation runs. The final prediction combined the individual predictions with a true skill statistic larger than or equal to 0.7 (57). The output of this prediction is a continuous variable that can range from zero to one for a given location in Europe. To better integrate the suitability map with the needs of the disease-spread simulation, the continuous scores were downscaled from the 5-km resolution to a 1-km resolution by using bilinear interpolation. This ensures that unsuitable barriers such as waterbodies are accurately accounted for when simulating spread. Furthermore, this improves the coverage of the predicted area in coastal areas with irregular shapes such as in Greece, which is crucial as many of the olive cells are located near the coast. Lastly, the downscaled map was converted into a binary prediction (suitable or unsuitable) for each 1- by 1-km cell using three different thresholds. Threshold 1 (0.165) is particularly informative for models based on presence-only data and ensures that a correct prediction on species presence of at least 90% is made. Threshold 2 (0.132) was used to maximize the sum of the accuracy of predicting occupied sites to be suitable and unoccupied sites to be unsuitable (i.e., sum of sensitivity and specificity); and 0.093 (T3) was used to minimize the difference between the accuracy of predicting occupied sites to be suitable and unoccupied sites to be unsuitable (i.e., minimum difference between sensitivity and specificity) (58).

Disease-Spread Simulation. Data on the olive-production sites in Europe were obtained from the CORINE land-cover map (https://land.copernicus.eu/pan-european/corine-land-cover) and aggregated to a 1-km resolution to reduce the computational time. To simulate spread, we used a basic radial range expansion model proposed for risk analyses in ref. 59. The model is the mathematical solution of a two-dimensional population growth model (exponential or logistic) with random dispersal, alias the Skellam model (60–62). Despite the model's simplicity, past population expansions have been found to compare reasonably well to such a radial range-expansion approach (63). The model has a single parameter called the rate of radial range expansion (*rr*), which depends on population growth and dispersal characteristics which are collapsed into a single parameter. For the value of *rr*, we used the 5%, 50%, and 95% quantiles of a distribution elicited from experts using formal methods for EKE (16). The quantiles correspond to radial rates of range expansion of 1.10, 5.18, and 12.35 km per year. The structured EKE followed the methodology described in the European Food Safety Authority Guidance on Uncertainty (64). Our concise overview of the approach follows the description in ref. 65. The ad hoc group included experts who defined the methodology as well as internationally recognized experts on the disease and on relevant agricultural practices. First, the parameter was reviewed, and clarifications were provided to the experts if needed. Second, evidence was provided and discussed to derive a list of evidence and uncertainties. The corresponding evidence table is published in ref. 16. Third, overall uncertainties were summarized. Fourth, the parameter was elicited by a structured expert judgement following the Quartile Method of the Sheffield protocol (66). Here, each of the seven invited experts was asked to individually estimate the following quantiles in this order: 1) 1st and 99th percentile, 2) median value, and 3) interquantile ranges. Afterward, estimates were discussed, and a consensus distribution was agreed upon by the group. Lastly, the fitted distribution was reviewed and agreed upon. In this EKE, the rate of radial range expansion was defined as the mean distance (kilometers) which will comprise 90% of the area containing the newly infected plants around an infected area within 1 y (16). Assumptions focused on disease spread by infected vectors, due to their natural dissemination or human-assisted movements, but not plant movements for trade. The estimates consider the heterogeneity of the European territory and the differences in vector abundance, as well as current control measures.

Radial range expansion was modeled by using a cellular automaton model with mixed neighborhood sequences (rook and queen) to generate cell-to-cell spread on a grid of 1- by 1-km cells. For this purpose, the discrete annual time steps were further broken down into within-year time steps. The number of within-year time steps depends on *rr*. For example, a rate of 5.18 km per year is approximated by 41 y of five and 9 y of six within-year time steps. This generates 259 steps in total and 5.18 steps per year on average. The ordering of the number of within-year steps across years was randomized. By ensuring that a proportion of $2-\sqrt{2}$ of steps were

taken in rook's fashion and $\sqrt{2}-1$ in queen's fashion, a spread pattern was generated which conformed to a regular octagon which closely encloses a circle (67). The step type (rook or queen) was randomly assigned to every step while ensuring that, over the course of the time horizon, the aforementioned proportions of rook and queen steps were obtained exactly. As corners of the octagon marginally overestimate spread, the area infected at every time step was constrained by a radial range model with the radius expanding at the elicited rate. Invasion into a cell was only accepted if it was climatically suitable, which ensured that unsuitable territories were not traveled through.

Economic Model. To account for economic differences between the countries and cropping systems, it was decided to stratify the population into *I* cropping systems indexed with *i* in *C* countries indexed with *c*. The total olive-growing area in Europe (A_0) was assumed to be constant at 4.6 million hectares for the entire planning horizon of 50 y (68). A planning horizon of 50 y was chosen due to the slow development of olive orchards as well as their natural longevity. The percentage distribution of the area of production into density (<140, 140 to 399, and >400 trees per hectare) and age (<5, 5 to 11, 12 to 49, and >50 y) classes for all countries was obtained from Eurostat (68). Additionally, Eurostat information on the national percentage of irrigated olive hectares was obtained. The density classes were further subdivided into rainfed and irrigated on the assumption that the irrigated share was the same across density classes. Within age classes, hectares were uniformly distributed. A dynamic model was built and run over a planning horizon of *T* years at an annual time step indexed by *t*. Orchard age was indexed by *a*. The area of production for country *c*, cropping-system *i*, of age *a* is denoted A_{cia}. Once the maximum longevity was reached, it was assumed that replanting is undertaken in the following year.

The prices are denoted (p_{ct}). Future monetary flows were discounted by the discount rate *r*. The replanting costs (RC_i) were accounted for by equivalent annual costs (ARC_i). Eq. **1** converts the establishment costs of an orchard to annual costs in dependence of the different longevities (m_i) of the evaluated cropping systems.

$$ARC_i = \frac{RC_i \cdot r}{1-(1+r)^{-m_i}}. \quad [1]$$

Yield in tons per hectare is specific for the country, cropping system, and tree age (Y_{cia}). We used cropping-system-specific information on full-bearing ages and full-bearing yield potential to linearly interpolate yield for all tree ages. Succeeding, we rescaled yields such that the simulated total production equals the 5-y averages prior to the detection of the pathogen (2007 to 2013) after FAOstat data. This equated to around 3.19 million, 2.37 million, and 6.69 million tons in Italy, Greece, and Spain, respectively. The yield was multiplied with the price (p_{ct}) to get the yearly revenue per hectare. The country, cropping system, and orchard age-specific operating costs (C_{cia}) as well as the equivalent annual costs for replanting (ARC_i) were subtracted from the revenue to obtain the profit (π_{ciat}) in Euros per hectare. Inner products of A_{cia} and π_{ciat} were computed to obtain the annual profit flow for the particular cropping system in country *c* and year *t* ($\mathbf{\Pi}_{cit}$). In other words, we multiplied the country, cropping system, and age-specific area with the corresponding profit and aggregated across all orchard ages. The total annual profit flows from olive production within Europe (Π_t) in year *t* was computed by summing the annual profit flows for all cropping systems across countries and across cropping systems. The net present values for the annual profit flows were obtained by discounting with the rate *r* by multiplying (Π_t) with $(1+r)^{-t}$.

The total production area affected by *Xfp* in country *c* at time *t* is denoted as A^x_{ct} and was obtained by the spread simulations in percent of the total national olive cells. The susceptible but disease-free area (Sx_{cit}) for cropping system *i*, country *c*, orchard age *a* at time *t* was calculated by subtracting the total area affected in year *t* from the total area (A_{cia}). The inner products of Sx_{cit} and the π_{ciat} were computed to obtain the annual profit flow of disease-free hectares for the particular cropping system (Π^h_{cit}). In other words, the area across orchards ages within a given country and cropping system was multiplied with the corresponding profits, and the resulting profits were aggregated over all orchard ages.

To store the disease progression within infected trees, tensors ($\mathbf{M}^x_{cit_x}$) were generated in which rows depict the different orchard ages, columns depict different points in time, and each element depicts the vector of different ages of infection. We denote by ΔA^x_{ct} the area of olives that was newly found to be infected in country *c* in year *t*, calculated by the difference of the cumulative percentage infected in succeeding discrete time steps. The newly infected area for cropping system *i*, country *c*, orchard age *a* in year *t*, was obtained by multiplying the percent of newly infected cells with the total number of hectares for the particular combination. The yield of infected orchards (Y^x_{cia,a_x}) declines with every discrete time step under infection (a_x). The country, cropping system, and age-of-infection-specific operating costs (C^x_{ci,a_x}) as well as the equivalent annual costs for replanting (ARC_i) were subtracted from the revenue to obtain the profit in Euros per hectare ($\pi^x_{cia_x}$). Orchards remain in production as long as their profit margins are nonnegative. Thenceforth, it was assumed that the production ceases, and no profit is generated from the infected orchards. Inner products of the ΔA^x_{ct} and the $\pi^x_{cia_x}$ were computed to obtain the annual profit flow of infected hectares for the particular cropping system (Π^x_{cit}). In other words, the infected area across orchard ages within a given country and cropping system was multiplied with the corresponding profits under infection, and the resulting profits were aggregated over all orchard ages.

As most of the orchards die off prematurely compared to the natural production cycles, additional costs arise due to the loss of investment. For an orchard of age *a* at the point of death, the farmer will have utilized *a* periods of the equivalent annual replanting costs. If orchards die before their maximum longevity (m_i) is reached, the system-specific equivalent annual replanting costs for the remainder of periods were accounted for as losses of the investment (L_{ia}) (Eq. **2**). To compute all possible losses of investment, vectors for all combinations of cropping system (*i*) and orchard age (*a*) were generated ($\mathbf{LI}_i$). The inner products of the died-off population ($\mathbf{v}^d_{cit}$) and $\mathbf{LI}_i$ were computed to obtain the total amount of lost investments in year *t* ($\mathbf{L}_{cit}$). In other words, the area of unprofitable orchards across orchards' ages within a given country and cropping system was multiplied with the corresponding losses in investment, and the resulting losses were aggregated over all orchard ages.

$$L_{ia} = [ARC_i \cdot (m_i - a)]. \quad [2]$$

To model a price response following the decrease in European supply, we computed the reduction in supply in percent (ΔQ) at the end of every time step. Subsequently, prices were updated by adding ($\Delta Q \times pr \times p_{ct}$), and profits ($\pi_{ciat}$ and $\pi^x_{cia_x}$) were recomputed for use in the following year. To estimate the price-response parameter (*pr*), we collected panel data from FAOstat on produced quantities of olives, the area of production, and price indices for Italy, Spain, and Greece from 1991 to 2017. As prices may influence the produced quantities and vice versa, parameter estimates obtained from ordinary least squares would suffer from endogeneity bias. We addressed this problem by instrumenting the produced quantities with the area of production. We estimated Eq. **3**, where log(*P*) and log(*Q*) are log-transformed prices and produced quantities, respectively. *Year* represents a time-trend, *Country* dummy variables for country effects, and $\log(P_{t-1})$ a lag to control for autocorrelation. τ, θ, ρ and β are parameters to be estimated, and ϵ is the independent and identically distributed error term. The coefficient (β) of log(*Q*) (-0.52, $P < 0.001$) was used as an estimate for the price-response parameter in our model.

$$\log(P) = \tau Year + \theta Country + \rho \log(P_{t-1}) + \beta \log(Q) + \epsilon. \quad [3]$$

To obtain the total annual profit flows from olive production within Europe in year *t* under the *Xfp* epidemic, all profits from disease-free (Π^h_{cit}) and infected (Π^x_{cit}) hectares are to be considered as well as the losses of investment ($\mathbf{L}_{cit}$). For the total annual profit flow (Π^x_t), it was aggregated across countries and cropping systems and discounted with rate *r* (Eq. **4**).

$$\Pi^x_t = \sum_{c=1}^{C}\sum_{i=1}^{I}[\Pi^h_{cit} + \Pi^x_{cit} - \mathbf{L}_{cit}] \cdot (1+r)^{-t}. \quad [4]$$

We denote by ΔA^r_{cit} the area of olives that is newly replanted in year *t*. The areas of replanted orchards are denoted A^r_{cit,a_r}. The yield and profit were assumed to be similar to the susceptible equivalents. For the best-case economic scenario, the total annual profit flows in year *t* under the *Xfp* epidemic is obtained by considering profits from disease-free (Π^h_{cit}), infected (Π^x_{cit}), and resistant (Π^r_{cit}) hectares, as well as the losses of investment ($\mathbf{L}_{cit}$). For the total annual profit flow (Π^r_t), it was aggregated across countries and cropping systems and discounted with rate *r* (Eq. **5**).

$$\Pi^r_t = \sum_{c=1}^{C}\sum_{i=1}^{I}[\Pi^h_{cit} + \Pi^x_{cit} + \Pi^r_{cit} - \mathbf{L}_{cit}] \cdot (1+r)^{-t}. \quad [5]$$

Economic impact for both scenarios (EI^x and EI^r) was computed by aggregating the differences between the profit flows without *Xfp* and profit flows Π^x_t and Π^r_t over *T*. The difference between Π^x_t and Π^r_t is expected to provide an exploration of the potential economic benefit associated with ongoing

research on resistance traits (*RB*). While EI^x, EI^r, and *RB* will depend on the choice of *T*, the discounting effect in the later years of the time horizon will result in only small differences if the number of years is slightly reduced or increased.

Global Sensitivity Analysis. To assess the parameter sensitivity, we conducted a global sensitivity analysis using a variance decomposition method (69). Sensitivity indices report the variance in the output *Y* attributable to variation in input X_i (first-order indices) as well as through higher-order interactions between this variable and other inputs (e.g., second-order indices). The total effect on the output caused by the input X_i is called the "total-order sensitivity index" (70). The conditional variance of input X_i and model output *Y* can be written as $V_{X_i}(E_{X_{\sim i}}(Y|X_i))$, with $X_{\sim i}$ denoting the matrix of all inputs except X_i. The inner expectation operator is the mean of output *Y* taken over all possible values of the input matrix except X_i. The outer variance is taken over all possible values of X_i. This is generally referred to as the "top marginal variance" of input X_i (71). The top marginal variance determines the reduction in output variation if the input is fixed with the true value. In contrast, $E_{X_{\sim i}}(V_{X_i}(Y|X_{\sim i}))$ is the expected variance that would remain if all inputs except X_i would be fixed. This is generally referred to as the "bottom marginal variance". The first-order sensitivity indices are bound between 0 to 1 and provide a measure of relative importance, with higher values implying larger effects on the outcome. The first-order sensitivity indices (S_i) and the total-order sensitivity indices (S_{Ti}) can be obtained by the following equations (71):

$$S_i = \frac{V_{X_i}(E_{X_{\sim i}}(Y|X_i))}{V(Y)}, \quad [6]$$

$$S_{Ti} = \frac{E_{X_{\sim i}}(V_{X_i}(Y|X_{\sim i}))}{V(Y)} = 1 - \frac{V_{X_{\sim i}}(E_{X_i}(Y|X_{\sim i}))}{V(Y)}. \quad [7]$$

First-order and total-order indices were computed after Sobol (72). To sample the input parameter space, 10,000 draws were generated from each input distribution. The computational time was improved by applying the Saltelli (70) sampler, which generated an input matrix of length $N(k+2)$, where *N* is the number of draws and *k* is the number of model inputs. The implementation used the improved formulas of refs. 71 and 73. In total, 31 parameters were included, which resulted in 330,000 rows of input values for which economic impact was computed by using one spread model (T2–RR50 in Italy).

Economic Data. A detailed overview is provided in the *SI Appendix*, Table S1. Prices and costs for olives in Euros per ton were obtained from ref. 47 with average prices in 2000 to 2009 of 481 and 497 Euros in Spain and Italy, respectively. The average costs of 247 and 316 Euros per ton for Spain and Italy comprise specific costs (fertilizers, crop protection, fuel, water, and other specific costs), farming overheads (building and machinery upkeep, energy, contract work, and other direct costs), depreciation, and external factors (wages, rent, and interest). Prices of Spain were above Italian prices from 2000 to 2005. Since then, Italian prices have been higher than Spanish prices. This might be related to the recent droughts in Italy. In addition, we might expect the higher prices to be related to (perceived) differences in product quality as well as the culinary focus of the Italian culture, which might result in consumers that are willing to pay more for their food products. Due to absence of published information on prices and costs from Greece, we consulted an expert, which resulted in an estimated price of 560 Euros and estimated costs of 387 Euros per ton. For the global sensitivity analysis, Italian prices (and costs) were sampled out of a normal distribution based on the computed means and SDs of 115 (53). The discount rate was set to 3% for the deterministic computation. For the global sensitivity analysis, the discount rate was sampled out of a uniform distribution between 3% and 7%, which comprises values frequently used in similar studies (74, 75). The prices were estimated to increase by 0.52% following a 1% decrease in supply. For the global sensitivity analysis, the estimated SD of 0.1 was used to sample out of a normal distribution.

There is uncertainty in the agronomical literature regarding the longevity of the different cropping systems. The effects of higher tree densities on the longevity of orchards is not yet fully understood (76). Rallo et al. (77) reported minimum values for the longevity of >100, >100, >40, >40, >20, and >15 y, for the rain-fed-traditional, irrigated-traditional, rain-fed-intensive, irrigated-intensive, rain-fed-high-density, and irrigated-high-density systems, respectively. Data from Eurostat suggest that around 23.47% and 0.68% of orchards in the density classes intensive and high density, respectively, are older than 50 y. To allow for the empirically observed ages within the different density classes, the longevities were set to 75 and 55 y for the intensive and high-density systems, respectively. To acknowledge the differences between cropping systems after Rallo et al. (77), the longevity of the traditional systems was set to 135 y for the deterministic computation. For the global sensitivity analysis, the longevities were sampled from uniform distributions ranging from 135 to 270, 75 to 150, and 55 to 110 for the traditional, intensive, and high-density systems, respectively.

The full-bearing tree ages were obtained from Rallo et al. (77). For the global sensitivity analysis, the ranges reported by Rallo et al. (77) were sampled out of a uniform distribution. The full bearing yield potential was obtained from Rallo et al. (77). For the global sensitivity analysis, the ranges reported by Rallo et al. (77) were sampled from a uniform distribution. The full-bearing ages and full-bearing yields were used to linearly interpolate the yields across ages. Succeeding, yields were rescaled to result in the empirically observed total production of olives according to FAOstat. For this, we made use of the 5-y averages (2007 to 2013) for Italy (3.19 million tons), Greece (2.37 million tons), and Spain (6.69 million tons). For the global sensitivity analysis, the estimated SD for Italian supply (2007 to 2013) was used to sample out of a normal distribution. The replanting costs in Euros per hectare were obtained from Rallo et al. (77) for the deterministic assessment. For the global sensitivity analysis, the uncertainty regarding possible costs for uprooting as well as geographic differences in replanting costs was approached by sampling uniformly between the reported costs and double the amount.

The annual yield decline due to *Xf* was set to 10%. The annual increase in cost due to *Xf* was set to 10%. For the global sensitivity analysis, the absence of knowledge on these parameters was approached by sampling out of a uniform distribution −5 to −50% and −25 to +25%, respectively.

Data Archival. All computations were performed on a high-performance computing cluster. Data and R scripts are available at https://doi.org/10.5281/zenodo.3672794.

ACKNOWLEDGMENTS. This work was supported by funding from the EU's Horizon 2020 Pest Organisms Threatening Europe research and innovation program under Grant 635646. M.C. held an Institut Valencià d'Investigacions Agràries grant partially funded by the European Social Fund Comunitat Valenciana 2014–2020. We thank the European Food Safety Authority for the EKE on the spread rate, Donato Boscia for sharing his expertise on the pathosystem, Lia Hemerik for her input on the spread model, and the high-performance computing cluster of Wageningen University and Research (Anunna) for allowing us to perform all computations free of charge.

1. J. M. Wells *et al.*, *Xylella fastidiosa* gen. Nov., sp. nov: Gram-negative, xylem-limited, fastidious plant bacteria related to *Xanthomonas* spp. *Int. J. Syst. Bacteriol.* **37**, 136–143 (1987).
2. EFSA, Update of the *Xylella* spp. host plant database. *EFSA J.* **16**, e05408 (2018).
3. European Commission, "Commission database of host plants found to be susceptible to *Xylella fastidiosa* in the Union territory—update 9" (Report Ref. Ares(2017)3824160, European Commission, Brussels, Belgium, 2017).
4. D. L. Hopkins, A. H. Purcell, *Xylella fastidiosa*: Cause of Pierce's disease of grapevine and other emergent diseases. *Plant Dis.* **86**, 1056–1066 (2002).
5. S. Chatterjee, P. Rodrigo, P. Almeida, S. Lindow, Living in two worlds: The plant and insect lifestyles of *Xylella fastidiosa*. *Annu. Rev. Phytopathol.* **46**, 243–271 (2008).
6. D. Cornara, D. Bosco, A. Fereres, *Philaenus spumarius*: When an old acquaintance becomes a new threat to European agriculture. *J. Pest. Sci.* **91**, 957–972 (2018).
7. D. L. Hopkins, *Xylella fastidiosa*: Xylem-limited bacterial pathogen of plants. *Annu. Rev. Phytopathol.* **27**, 271–290 (1989).
8. European Food Safety Authority, Scientific opinion on the risk to plant health posed by *Xylella fastidiosa* in the EU territory, with the identification and evaluation of risk reduction options. *EFSA J.* **13**, 3989 (2015).
9. M. Saponari *et al.*, Isolation and pathogenicity of *Xylella fastidiosa* associated to the olive quick decline syndrome in southern Italy. *Sci. Rep.* **7**, 17723 (2017).
10. A. Purcell, Paradigms: Examples from the bacterium *Xylella fastidiosa*. *Annu. Rev. Phytopathol.* **51**, 339–356 (2013).
11. M. Saponari *et al.*, Pilot project on *Xylella fastidiosa* to reduce risk assessment uncertainties. *EFSA Supporting Publ.* **13**, 1013E (2016).
12. R. P. P. Almeida, Can Apulia's olive trees be saved?*Science* **353**, 346–348 (2016).
13. E. Stokstad, Food security: Italy's olives under siege. *Science* **348**, 620 (2015).
14. C.-C. Su, Pierce's disease of grapevines in Taiwan: Isolation, cultivation and pathogenicity of *Xylella fastidiosa*. *J. Phytopathol.* **161**, 389–396 (2013).
15. G. Strona, C. J. Carstens, P. S. A. Beck, Network analysis reveals why *Xylella fastidiosa* will persist in Europe. *Sci. Rep.* **7**, 71 (2017).
16. C. Bragard *et al.*, Update of the scientific opinion on the risks to plant health posed by *Xylella fastidiosa* in the EU territory. *EFSA J.* **17**, e05665 (2019).
17. E. M. Bucci, *Xylella fastidiosa*, a new plant pathogen that threatens global farming: Ecology, molecular biology, search for remedies. *Biochem. Biophys. Res. Commun.* **502**, 173–182 (2018).

18. F. D. Serio *et al.*, Collection of data and information on biology and control of vectors of *Xylella fastidiosa*. *EFSA Supporting Publ.* **16**, 1628E (2019).
19. M. D. Pascali *et al.*, Molecular effects of *Xylella fastidiosa* and drought combined stress in olive trees. *Plants* **8**, 437 (2019).
20. Erika. Sabella *et al.*, *Xylella fastidiosa* induces differential expression of lignification related-genes and lignin accumulation in tolerant olive trees cv. Leccino. *J. Plant Physiol.* **220**, 60–68 (2018).
21. A. Baù, A. Delbianco, G. Stancanelli, S. Tramontini, Susceptibility of *Olea europaea* L. Varieties to *Xylella fastidiosa* subsp. pauca ST53: Systematic literature search up to 24 March 2017. *EFSA J.* **15**, 4772 (2017).
22. A. Luvisi, F. Nicoli, L. D. Bellis, Sustainable management of plant quarantine pests: The case of olive quick decline syndrome. *Sustainability* **9**, 659 (2017).
23. A. Luvisi *et al.*, *Xylella fastidiosa* subsp. pauca (CoDiRO strain) infection in four olive (*Olea europaea* L.) cultivars: Profile of phenolic compounds in leaves and progression of leaf scorch symptoms. *Phytopathol. Mediterr.* **56**, 259–273 (2017).
24. R. Caserta, R. R. Souza-Neto, M. A. Takita, S. E. Lindow, A. A. D. Souza, Ectopic expression of *Xylella fastidiosa* rpfF conferring production of diffusible signal factor in transgenic tobacco and citrus alters pathogen behavior and reduces disease severity. *Mol. Plant Microbe Interact.* **30**, 866–875 (2017).
25. A. Giampetruzzi *et al.*, Transcriptome profiling of two olive cultivars in response to infection by the CoDiRO strain of *Xylella fastidiosa* subsp. pauca. *BMC Genom.* **17**, 475 (2016).
26. I. Kyrkou, T. Pusa, L. Ellegaard-Jensen, M.-F. Sagot, L. H. Hansen, Pierce's disease of grapevines: A review of control strategies and an outline of an epidemiological model. *Front. Microbiol.* **9**, 2141 (2018).
27. C. Baccari, E. Antonova, S. Lindow, Biological control of Pierce's disease of grape by an endophytic bacterium. *Phytopathology* **109**, 248–256 (2019).
28. European Commission, Commission implementing decision 2017/2352 amending implementing decision 2015/789 as regards measures to prevent the introduction into and the spread within the union of *Xylella fastidiosa* (Wells et al.). *Official J.* **L336**, 31–44 (2017).
29. K. Schneider, M. Cendoya, J. Navas-Cortes, Data and R scripts for "Impact of Xylella fastidiosa subspecies pauca in European Olives." Zenodo. http://doi.org/10.5281/zenodo.3672794. Deposited 18 February 2020.
30. Eurostat , *Agriculture, Forestry and Fishery Statistics* (Eurostat, Luxembourg, 2016).
31. S. M. White, J. M. Bullock, D. A. P. Hooftman, D. S. Chapman, Modelling the spread and control of *Xylella fastidiosa* in the early stages of invasion in Apulia, Italy. *Biol. Invasions* **19**, 1825–1837 (2017).
32. T. P. Holmes, J. E. Aukema, B. Von Holle, A. Liebhold, E. Sills, Economic impacts of invasive species in forests. *Ann. N. Y. Acad. Sci.* **1162**, 18–38 (2009).
33. M. Saponari, A. Giampetruzzi, G. Loconsole, D. Boscia, P. Saldarelli, *Xylella fastidiosa* in olive in Apulia: Where we stand. *Phytopathology* **109**, 175–186 (2019).
34. European Commission, Commission implementing decision 2015/789 as regards measures to prevent the introduction into and the spread within the union of *Xylella fastidiosa* (Wells et al.). *Off. J.* **L125**, 36 (2015).
35. A. Fierro, A. Liccardo, F. Porcelli, A lattice model to manage the vector and the infection of the *Xylella fastidiosa* on olive trees. *Sci. Rep.* **9**, 8723 (2019).
36. A. Hafi, L. Randall, T. Arthur, D. Addai., P. Tennant, J. Gomboso, "*Economic impacts of Xylella fastidiosa on the Australian wine grape and wine-making industries*" (Report, Australian Department of Agriculture, Canberra City, Australia, 2017).
37. M. S. Sisterson, D. C. Stenger, Roguing with replacement in perennial crops: Conditions for successful disease management. *Phytopathology* **103**, 117–128 (2013).
38. A. O. Lansink, Public and private roles in plant health management. *Food Pol.* **36**, 166–170 (2011).
39. K. M. Rich, G. Y. Miller, A. Winter-Nelson, A review of economic tools for the assessment of animal disease outbreaks. *Revue Sci. Et Tech. Off. Int. Epizoot.* **24**, 833–845 (2005).
40. T. Soliman, M. C. M. Mourits, A. G. J. M. Oude Lansink, W. van der Werf, Economic justification for quarantine status—the case study of '*Candidatus Liberibacter solanacearum*' in the European Union. *Plant Pathol.* **62**, 1106–1113 (2013).
41. D. C. Cook, R. W. Fraser, Trade and invasive species risk mitigation: Reconciling WTO compliance with maximising the gains from trade. *Food Pol.* **33**, 176–184 (2008).
42. M.-J. J. Mangen, A. M. Burrell, Who gains, who loses? Welfare effects of classical swine fever epidemics in The Netherlands. *Eur. Rev. Agric. Econ.* **30**, 125–154 (2003).
43. T. T. Assefa, M. P. M. Meuwissen, A. G. J. M. Oude Lansink, Price volatility transmission in food supply chains: A literature review. *Agribusiness* **31**, 3–13 (2015).
44. M. Cutts, J. Kirsten, Asymmetric price transmission and market concentration: An investigation into four South African agro-food industries. *S. Afr. J. Econ.* **74**, 323–333 (2006).
45. European Commission, *Economic Analysis of the Olive Sector* (Directorate-General for Agriculture and Rural Development, Brussels, Belgium, 2012).
46. Eurostat, *Economic accounts for Agriculture—Values at Current Prices* (Eurostat, Luxembourg, 2019).
47. European Commission, :EU olive oil farms report" (Report, Directorate-General for Agriculture and Rural Development, Brussels, Belgium, 2012).
48. G. N. Agrios, *Plant Pathology* (Academic Press, New York, NY, ed. 5, 2005).
49. M. S. Sisterson, D. C. Stenger, Modelling effects of vector acquisition threshold on disease progression in a perennial crop following deployment of a partially resistant variety. *Plant Pathol.* **67**, 1388–1400 (2018).
50. A. Guisan, N. E. Zimmermann, Predictive habitat distribution models in ecology. *Ecol. Model.* **135**, 147–186 (2000).
51. A. T. Peterson *et al.*, *Ecological Niches and Geographic Distributions* (Princeton University Press, Princeton, NJ, 2011).
52. EPPO Reporting Service, "*X. Fastidiosa subsp. multiplex detected in Toscana region in November 2018*" (Report, EPPO Reporting Service 2019/016, European and Mediterranean Plant Protection Organization, Paris, France, 2019).
53. EPPO Reporting Service, "*Xylella fastidiosa* subsp. multiplex was first found in December 2018 on lavender plants (in a zoo garden) in the municipality of Vila Nova de Gaia (near Porto)" (Report, EPPO Reporting Service 2019/017, European and Mediterranean Plant Protection Organization, Paris, France, 2019).
54. EPPO Reporting Service, "Detected for the first time in 2019 in symptomatic almond trees in 3 adjacent commercial orchards in the Hula Valley (Northeastern Part). Laboratory analysis confirmed the presence of *X. fastidiosa* subsp. Fastidiosa" (Rep. 2019/121, European and Mediterranean Plant Protection Organization, Paris, France, 2019).
55. D. N. Karger, Climatologies at high resolution for the earth's land surface areas. *Sci. Data* **4**, 170122 (2017).
56. O. Allouche, A. Tsoar, R. Kadmon, Assessing the accuracy of species distribution models: Prevalence, kappa and the true skill statistic (TSS). *J. Appl. Ecol.* **43**, 1223–1232 (2006).
57. A. Guisan., W. Thuiller, N. E. Zimmermann, *Habitat Suitability and Distribution Models* (Cambridge University Press, Cambridge, UK, 2017).
58. A. Jiménez-Valverde, J. M. Lobo, Threshold criteria for conversion of probability of species presence to either–or presence–absence. *Acta Oecol.* **31**, 361–369 (2007).
59. C. Robinet *et al.*, A suite of models to support the quantitative assessment of spread in pest risk analysis. *PloS One*, **7**, e43366 (2012).
60. J. G. Skellam, Random dispersal in theoretical populations. *Biometrika* **38**, 196–218 (1951).
61. A. Okubo, S. A. Levin, *Diffusion and Ecological Problems: Modern Perspectives (Interdisciplinary Applied Mathematics*, Springer, New York, NY, 2001), vol. 14.
62. N. Shigesada, K. Kawasaki, *Biological Invasions: Theory and Practice* (Oxford University Press, New York, NY, ed. 1, 1997).
63. E. J. Hudgins, A. M. Liebhold, B. Leung, Predicting the spread of all invasive forest pests in the United States. *Ecol. Lett.* **20**, 426–435 (2017).
64. D. Benford *et al.*, Guidance on uncertainty analysis in scientific assessments. *EFSA J.* **16**, 5123 (2018).
65. R. Baker *et al.*, Report on the methodology applied by EFSA to provide a quantitative assessment of pest-related criteria required to rank candidate priority pests as defined by Regulation (EU) 2016/2031. *EFSA J.* **17**, 5731 (2019).
66. European Food Safety Authority, Guidance on expert knowledge elicitation in food and feed safety risk assessment. *EFSA J.* **12**, 3734 (2014).
67. J. Farkas, S. Bajk, B. Nagy, Approximating the Euclidean circle in the square grid using neighbourhood sequences. *Pure Math. Appl.* **17**, 309–322 (2006).
68. Eurostat, *Olive Trees—Area by Age and Density Classes* (Eurostat, Luxembourg, 2019).
69. A. Saltelli *et al.*, *Global Sensitivity Analysis. The Primer* (John Wiley & Sons, Ltd, Chichester, UK, 2007).
70. A. Saltelli, Making best use of model evaluations to compute sensitivity indices. *Comput. Phys. Commun.* **145**, 280–297 (2002).
71. A. Saltelli, Variance based sensitivity analysis of model output. Design and estimator for the total sensitivity index. *Comput. Phys. Commun.* **181**, 259–270 (2010).
72. I. M. Sobol, Global sensitivity indices for nonlinear mathematical models and their Monte Carlo estimates. *Math. Comput. Simulat.* **55**, 271–280 (2001).
73. M. J. W. Jansen, Analysis of variance designs for model output. *Comput. Phys. Commun.* **117**, 35–43 (1999).
74. J. M. Alston, K. B. Fuller, J. D. Kaplan, K. P. Tumber, Economic consequences of Pierce's disease and related policy in the California winegrape industry. *J. Agric. Resour. Econ.* **38**, 269–297 (2013).
75. K. P. Tumber, J. M. Alston, K. B. Fuller, *The costs of Pierce's disease in the California winegrape industry* (CWE Working Paper 1204, Robert Mondavi Institute Center for Wine Economics, University of California, Davis, CA, 2012).
76. C. M. Díez *et al.*, Cultivar and tree density as key factors in the long-term performance of super high-density olive orchards. *Front. Plant Sci.* **7** 1226 (2016).
77. L. Rallo, D. Barranco, S. Castro-García, D. J. Connor, "María Gómez del Campo, and Pilar Rallo. high-density olive plantations" in *Horticultural Reviews*, J. Janick, Ed. (John Wiley & Sons, Inc., Hoboken, NJ, 2014), vol. 41, pp. 303–384.